PROCEEDINGS OF SCIENCE

ONLINE ICRC 2021 THE ASTROPARTICLE PHYSICS CONFERENCE Berlin | Germany
37th International Cosmic Ray Conference 12–23 July 2021

Sensitivity of the Tibet hybrid experiment (Tibet-III + MD) for primary proton spectrum between 30 TeV and a few hundreds of TeV's

D. Kurashige,[a,*] D. Chen,[b] N. Hotta,[c] J. Huang,[d] Y. Katayose,[a] K. Kawata,[e] M. Ohnishi,[e] T. Saito,[f] T. K. Sako,[e] M. Shibata[a] and M. Takita[e]

[a] *Faculty of Engineering, Yokohama National University, Yokohama, Japan*
[b] *National Astronomical Observatories, Chinese Academy of Sciences, Beijing, China*
[c] *Faculty of Engineering, Utsunomiya University, Utsunomiya, Japan*
[d] *Key Laboratory of Particle Astrophysics, Institute of High Energy Physics, Chinese Academy of Sciences, Beijing, China*
[e] *Institute for Cosmic Ray Research, University of Tokyo, Kashiwa, Japan*
[f] *Tokyo Metropolitan College of Industrial Technology, Tokyo, Japan*

E-mail: kurashige-daichi-ts@ynu.jp

In the Tibet ASγ experiment, continuous observation of cosmic rays and cosmic gamma rays from TeV to tens of PeV has been carried out using a hybrid detector that combines the air shower detector array (Tibet-III) and the water Cherenkov muon detector array (MD). To measure the proton spectrum from 30 TeV to 400 TeV, we developed a proton-shower selection method using the difference of the number of muons in the air shower depending on the primary nuclide. In the Monte Carlo simulations to evaluate the performance of this method, we used a Heavy-dominant model in which the proportion of heavy nuclei in the "knee" region gradually increases and a Helium-rich model in which the proportion of Helium gradually increases as the primary cosmic ray chemical composition model, and the QGSJET-II-04 and the SIBYLL 2.3c were used as the shower interaction models. This method made it possible to select protons with a purity of 90%, and the detection efficiency of protons was approximately 17.8% at 30 TeV and 8.6% at 400 TeV respectively. The energy resolution of the selected protons was approximately 53% at 30 TeV and 27% at 400 TeV respectively. The total systematic error of the proton flux depending on these models was found to be approximately ±36%. These results indicate that the new hybrid measurement method is powerful enough to study the proton spectrum in the knee region.

37th International Cosmic Ray Conference (ICRC 2021)
July 12th – 23rd, 2021
Online – Berlin, Germany

*Presenter

1. Introduction

The origin of cosmic rays up to around the PeV region is generally thought to be in our galaxy. X-ray [1, 2] and TeV gamma-ray [3] observations from shell-type SNR revealed that electrons are accelerated by diffusive shock acceleration [4] in shock waves [5, 6]. For protons, which occupy most of the cosmic rays, observations of gamma ray from SNR [7–9] have obtained energy spectra thought to be of neutral pion origin, and evidence of hadronic particle acceleration has been accumulating. The maximum energy of a particle in the standard SNR shock-wave model is several hundred TeV for protons, however, observation of TeV gamma rays by the H.E.S.S. group indicated that there may be a source that accelerates protons above PeV ("PeVatron") in the galactic center [10]. Observations of diffuse gamma rays in the 100 TeV region [11] also suggest that a PeVatron existed in the past or present. The debate are still ongoing, such as how large is the maximum energy of galactic cosmic ray sources and what is PeVatron.

Acceleration mechanisms and source distribution have an influence on cosmic-ray chemical composition and intensity spectrum observed on the earth, especially the bending shape of the total particle spectrum around 10^{15}eV ("knee"), which is considered to be caused by the acceleration limit of galactic cosmic rays. Therefore, the measurement of the composition and spectra around the knee region are important to clarify the acceleration mechanism and propagation. In the lower energy side of the knee, from 10^{12}eV to 10^{14}eV, the high precision spectrum of protons have been obtained by balloon and satellite experiments [12–15], and contrary to expectations, it turned out that the power of the spectrum shape becomes hard from around 10^{12} eV [16]. To explain this, theoretical models such as the influence from a source object near our solar system have been proposed, but have not been clarified until now. On the high-energy side, where indirect observation using an air shower is required, definitive observation results of the spectrum have not been obtained. For example, the Tibet ASγ reported that the proton spectral index changes over several hundred TeV [17, 18], pointing to a rigidity dependent acceleration model in which heavier nuclei gradually become dominant. On the other hand, observation results in which helium is dominant [19] and measurement results in which the power index of the proton spectrum is hard up to the PeV region [20] have also been reported. The region between tens of TeV and hundreds of TeV, which is in the middle of the energy region, is between the upper energy limit of direct observation due to the lower event frequency and the energy of effective ground observation, and new precise measurements with high statistics of composition and spectrum are demanded.

One of the difficulties in composition measurements using air showers is the identification of incident nuclides. To separate incident nuclides, two kinds of characteristics in an air shower are often used. One is the difference in shower development due to the interaction cross-section of the nuclides. The Tibet ASγ group measured the light nuclei components in the knee region using a primary separation method that used the difference in the spread of high-energy particles in the center of the shower [21–24]. The other method is to measure muon and shower particle densities originating from nuclear interactions in the shower. The number of muons in an air shower is one of the powerful parameters for separating the mass numbers of incident particles. For particles with the same energy and different nuclides, the larger the mass number, the larger the number of muons produced in the decay process. Therefore, nuclear species can be selected using the number of charged particles and the number of muons as parameters. Some experimental groups have reported the cosmic-ray primary composition in the knee region through the air-shower electromagnetic and muon measurements [19, 25] .

We have been conducting a continuous observation to study cosmic-ray composition around the knee region in Tibet ASγ experiment. The detector consists the surface detector array (Tibet-III) [26, 27], the air-shower core detector array (YAC) and the large underground water Cherenkov muon detector (MD) [28, 29]. The MD was developed primarily for gamma-ray observations at tens of TeV and above and can remove about 70 percent of hadronic cosmic rays at 10 TeV. At 100 TeV, it becomes nearly background-free at about 99.92%, and gamma rays above 100 TeV from Crab have been reported [30]. MD is also effective for particle separation in nuclear showers. In particular, protons can be measured with high statistics by a measurement method that uses only the shower size and the number of muons. In this study, we developed a method to obtain proton spectrum from 30 TeV to 400 TeV by using the Tibet-III air-shower array in conjunction with the MD array and evaluated the measurement performance by Monte Carlo simulation.

2. Tibet-III air shower array and Muon Detector

The experimental site of Tibet ASγ is located on Yangbajing Plateau, China (90.522° east, 30.102° north, 4300 m a.s.l., 606 g/cm^2 atmospheric depth). The detector consists of the Tibet-III air-shower array [31], which consists of 597 plastic scintillation detectors, and the underground muon detector array (MD) [28, 29]. The Tibet-III array covers an area of 65700 m^2, it detects electromagnetic components such as electrons and gamma rays in air showers, and measures the particle arrival time and density of shower particles. With these data, the direction of arrival and the energy of the primary cosmic rays are reconstructed for each event. The Tibet MD array consists of 64 water Chelenkov type detectors placed 2.4 m beneath the Tibet-III array, each cell of the MD array is a concrete water tank 7.2 m $\times$ 7.2 m wide and 1.5 m deep, with a 20-inch diameter PMT mounted downward on the ceiling. The inner walls are covered with white Tyvek sheets to collect the Chelenkov light produced by the muons efficiently. The energy threshold for the muon to penetrate the soil is about 1 GeV.

3. Monte Carlo simulation of air shower and detector response

To reconstruct the primary cosmic rays from the data obtained by the Tibet-III and MD and calculate the spectra, it is necessary to clarify the detection efficiency and the ability of nuclide selection by Monte Carlo simulation. Furthermore, the uncertainty of the composition of cosmic rays used in the simulation itself may affect the bias of detection efficiency. Therefore, we performed Monte Carlo simulations of air-shower development assuming multiple combinations of the primary composition model and the nuclear cascade model of air shower, and simulated the detector response using the GEANT4.10.02 code. The CORSIKA code (version 7.6400) [32] was used for the air-shower simulations, and two interaction models were compared for the high energy region. The first is the SIBYLL 2.3c model [33, 34], which was developed based on the QCD mini-jet model. The second is the QGSJET-II-04 [35], which was developed based on the Gribov-Regge theory. In addition, the FLUKA model [36] was used for the low energy region. The following two models were compared as a chemical composition model of primary cosmic rays. The first is the "Shibata-model" [37], which is obtained by fitting the power function of energy to data of direct observations up to a few TeV and data of the Tibet ASγ experiment. In this model, heavier nuclei gradually dominate from the tens of TeV regions. The other model is the "Gaisser fit model" [38], which is obtained from observation results in which helium is the main component at 100 TeV and above. The two models match well up to 100 TeV, but the Gaisser fit model is the helium dominant above 100 TeV, and it gives stricter conditions for background helium rejection in proton selection using muon numbers.

4. MC data analysis

The values of the number of particles and their arrival timings by each surface detector were recorded in the same format as the experimental data and analyzed using the same procedure as in the experiment [31, 39, 40]. This analysis provides the core position, the arrival direction of the shower, and the number density of charged particles. Each cell in the MD array has a 20-inch diameter PMT mounted downward on the ceiling and the number of Chelenkov photons striking the PMT is calculated. The distribution of the number of photons when one muon is incident in the pool is examined, and the peak value of the distribution is defined as 1 MIP (minimum ionization particle). The number of muons in the pool for each MD is obtained by dividing the measured photon number by the value of the single peak.

4.1 Data selection

To screen well reconstructed shower events from the whole data detected in the array, the following conditions were imposed.

1. There are at least four detectors in the inner area of the array that detected at least 3.5 particles.
2. Five or more of the top 6 detectors with the highest number of detected particles are contained in the inner area.
3. The location of the air shower core determined by the analysis must be within a radius of 70 m from the array center.
4. The zenith angle θ satisfies $\sec\theta < 1.1$.
5. The residual error which is obtained by the same procedure as in the experiment must be less than 1.0 m.

5. Results and discussion

5.1 Proton selection with number of muons

Fig. 1(a) is a scatter plot of the charged particle number density $\Sigma\rho$ measured by Tibet-III and the number of muons in the shower N_μ measured by MD. This is the result of a shower event when SIBYLL/FLUKA is used as the interaction model and the Shibata-model is used for the cosmic ray chemical composition. The red plot shows protons and the gray plot shows nuclides heavier than protons. In the region where N_μ is large, protons are overlapped by heavier nuclides, i.e., protons and other particles are mixed. On the other hand, where N_μ is small, there is a region where only

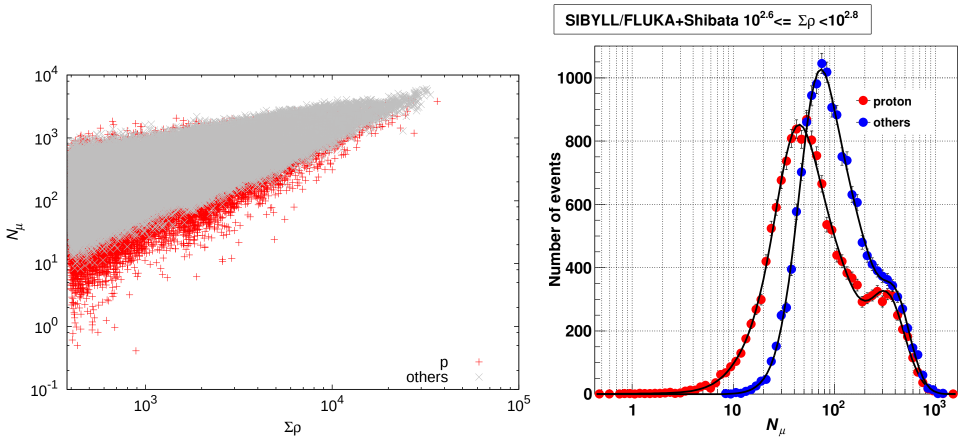

(a) **(b)**

Figure 1: (a) A scatter plot of the charged particle number density ($\Sigma\rho$) measured by Tibet-III and the number of muons (N_μ) in the shower measured by MD. This is the result of a shower event when SIBYLL/FLUKA is used as the interaction model and the Shibata-model is used for the cosmic ray chemical composition. The red plot shows protons and the gray plot shows nuclides heavier than protons. (b) Muon distribution for events with $10^{2.6} < \Sigma\rho < 10^{2.8}$. Red plots show protons, and blue plots show others. Each fit line is defined by Eq. (1).

protons are present. By selecting proton events in this region, it is possible to select only proton events with high purity.

To investigate the mixing ratio of protons and other particles, we divided the data in Fig. 1(a) into bins for $\Sigma\rho$ and examined the distribution of the number of muons in each bin. Fig. 1(b) shows the results for events with $10^{2.6} < \Sigma\rho < 10^{2.8}$, where the red plot is for protons and the blue plot is for heavy nuclei. The bumps seen in Fig. 1(b) at higher N_μ than peak position are due to the effect of geometrical configuration of MD. More number of muons are detected when shower core hits the MD pool than other cases. This effect is included as follows. The solid curve, F shows the equation obtained by fitting the sum of the following four Gaussian functions.

$$f_i = c_i \frac{1}{\sqrt{2\pi b_i}} \exp\left(-\frac{(\log(x) - a_i)^2}{\sqrt{2b_i^2}} \right) \quad , \quad F = \sum_{i=1}^{4} f_i \tag{1}$$

Using the F, the number of events of protons and other particles were summed up from the lowest muon number to obtain the $\Sigma\rho$ value $N_{\mu,cut}$ where the proportion of protons is 90% of the total. For this $\Sigma\rho$ bin, $N_{\mu,cut}$ was estimated to be approximately 26.31. This operation was performed for each $\Sigma\rho$ bin and each $N_{\mu,cut}$ was determined. The $N_{\mu,cut}$ values were fitted as a function of $\Sigma\rho$, and air shower events with N_μ smaller than this cut line were determined to be proton-like. The detection efficiency of protons was approximately 17.8% at 30 TeV and 8.6% at 400 TeV respectively.

5.2 Energy resolution

The energy distribution of the proton-like events in the $10^{2.6} < \Sigma\rho < 10^{2.8}$ bin is shown in Fig. 2. The blue plot is the result of the calculation, and the solid red line is the curve fitted with a function combining two different Eq. (1) around the peak. The energy of the peak of the distribution was taken as the representative energy of the $\Sigma\rho$ bin. Representative energy was determined for each bin and each representative energy was fitted as a function of $\Sigma\rho$ to obtain a conversion function for energy determination. The energy resolution of the proton-like events was approximately 53% at 30 TeV and 27% at 400 TeV respectively.

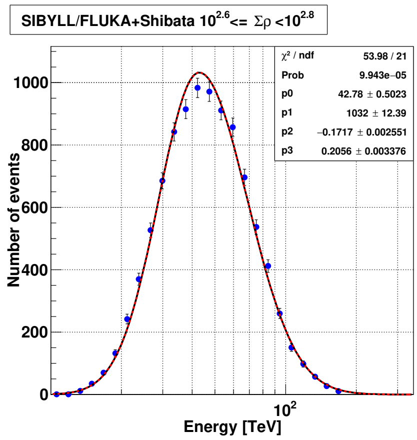

Figure 2: The energy distribution of the proton-like events in the $10^{2.6} < \Sigma\rho < 10^{2.8}$ bin.

5.3 Reconstructed energy spectrum of protons (MC)

The other three models (SIBYLL/FLUKA+Gaisser, QGSJET-II/FLUKA+Shibata, and QGSJET-II/FLUKA+Gaisser) were also analyzed using the same procedure as in section 5.1 and section 5.2. To investigate the systematic errors of the proton flux among these four models, the MC data of the SIBYLL/FLUKA+Shibata model was analyzed with the conditions obtained by each model. Fig. 3 shows the proton spectrum for each model. The systematic error is estimated to be up to ±36% between SIBYLL/FLUKA+Shibata and QGSJET-II/FLUKA+Gaisser.

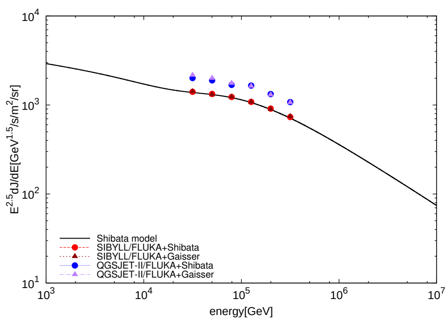

Figure 3: Reconstructed energy spectrum of protons (MC). Each plot show the result of analyzing SIBYLL/FLUKA+Shibata MC events with the analysis conditions obtained in the analysis of each model.

6. Summary

We developed a method to measure proton spectra using data obtained by hybrid measurement of Tibet-III and MD, and evaluated its performance. It was found that the proton spectrum can be measured in the energy range from 30 TeV to 400 TeV by selecting protons with a purity of 90%. The expected systematic error of the proton spectrum was found to be about ±36%. Using this method, we plan to analyze several years of data accumulated in the Tibet ASγ experiment to clarify the proton spectrum from 30 TeV to 400 TeV.

Acknowledgements

The collaborative experiment of the Tibet Air Shower Arrays has been conducted under the auspices of the Ministry of Science and Technology of China and the Ministry of Foreign Affairs of Japan. This work is supported by the joint research program of the Institute for Cosmic Ray Research (ICRR), the University of Tokyo.

References

[1] K. Koyama et al., Nature **378** (1995) 255

[2] Slane, P. et al, Astrophys. J., **525** (1999) 357

[3] T. Tanimori et al., Astrophys. J., **497** (1995) L25

[4] Bell, A. R., MNRAS, **182** (1978) 147

[5] Reynolds, S. P., Astrophys. J., **493** (1998) 375

[6] Reynolds, S. P., A&A, **46** (2008) 89

[7] M. Ackermann et al., SCIENCE **339** (2013) 807

[8] T. Jogler and S. Funk., ApJ, **816** (2016) 100

[9] M. Amenomori et al., Nature Astronomy, **5** (2021) 460

[10] A. Abramowski et al., Nature, **531** (2016) 476

[11] M. Amenomori, Phys. Rev. Lett., **126** (2021) 141101

[12] A. D. Panov et al., Bull. Russ. Acad. Sci.: Phys., **71** (2007) 494

[13] Y. S. Yoon et al., Astrophys. J., **839** (2017) 5

[14] O. Adriani et al., Phys. Rev. Lett., **122** (2019) 181102

[15] Q. An et al., Sci. Adv., **5** (2019) eaax3793

[16] N. Tomassetti, ApJ Lett. **752** (2012) L13

[17] M. Amenomori et al, Adv. Space Res., **42** (2008) 647

[18] M. Amenomori et al, ApJ, **678** (2008) 1165

[19] W.D. Apel et al, Astroparticle Phys. , **31** (2009) 86

[20] K. Rawlins, Phys. At. Nucl., **83** (2020) 280

[21] M. Amenomori et al, PHYSICS LETTERS B , **632** (2006) 58

[22] M. Amenomori et al, Adv. Space Res. , **37** (2006) 1938

[23] M. Amenomori et al, J. Phys. Soc. Jpn. Suppl. A , **78** (2009) 206

[24] M. Amenomori et al, Adv. Space Res., **47** (2011) 629

[25] M. Aglietta et al., Astroparticle Phys., **21** (2004) 583

[26] M. Amenomori et al., ApJ, **692** (2009) 61

[27] M. Amenomori et al., ApJ Lett., **709** (2010) L6

[28] T.K. Sako et al., Astroparticle Phys., **32** (2009) 177

[29] M. Amenomori et al., ApJ, **813** (2015) 98

[30] M. Amenomori et al., Phys. Rev. Rett., **123** (2019) 05113

[31] M. Amenomori et al., ApJ, **598** (2003) 242

[32] Heck D. et al., Forschungszentrum Karlsruhe Report FZKA 6019 (1998)

[33] R. Enge .et al. , EPJ Web of Conferences , **145** (2017) 08001

[34] A. Fedynitch .et al. , Phys. Rev. D, **100** (2019) 103018

[35] Ostapchenko S. , Nucl. Phys. B (Proc. Suppl.), **151** (2006) 143

[36] Battistoni G.et al. , Annals of Nuclear Energy, **82** (2015) 10

[37] M. Shibata et al., ApJ, **716** (2010) 1076

[38] T.K. Gaisser et al., Front. Phys., **8** (2013) 748

[39] M. Amenomori et al., Phys. Rev. Rett., **69** (1992) 2468

[40] Kawata, K et al, Exp. Astron. **44** (2017) 1